Metal-Metal Coupling and Metal-Ligand Interactions in Four Binuclear Complexes of Vanadium(I), -(II), and -(III). An ab Initio CI Study

Charles Poumbga, Chantal Daniel, and Marc Bénard*

Contribution from the Laboratoire de Chimie Quantique, E.R. 139 du CNRS, Institut Le Bel, F-67000 Strasbourg, France. *Received July 6, 1990*

Abstract: An iterative, multireference configuration interaction procedure in the spirit of the iterative natural orbital method of Bender and Davidson is defined and applied to four binuclear complexes of vanadium characterized by different oxidation states and formal V-V bond orders: $(C_5H_5\text{-}V)_2C_8H_8$ (**1**), $(C_5H_5\text{-}V\text{-}C_4H_8)_2$ (**2**), $(C_9H_7\text{-}V)_2$ (**3**), and $(C_5H_5\text{-}V\text{-}H)_2C_6H_6$ (**4**). The electronic structure of the complexes is first analyzed qualitatively from interaction diagrams based upon extended Hückel calculations. A rationalization of the metal-metal interactions is then presented, based upon the natural orbitals issued from the final CI expansions. Several types of metal-metal interactions are shown to be at work in these four complexes: δ antiferromagnetic couplings, direct V-V σ bonds, metal-ligand-metal delocalized interactions, and large V-V bonding contributions to ligand orbitals. These various kinds of V-V coupling may coexist in the same molecule and deeply alter the formal bonding scheme that can be deduced from electron-counting considerations. The practical result is an equalization of the characters and properties of the dimetal fragment: the net metal charges, the singlet-triplet energy separations, and the computed V-V bond orders appear to be strikingly similar for all considered complexes. These similarities are consistent with the narrow range of the observed V-V distances and suggest that the metal-ligand interactions represent the driving force conditioning the structure and properties of the dimetal subunit.

The nature of the metal-metal coupling in binuclear complexes of vanadium has been the subject of several theoretical studies in recent times.[1-6] Cotton et al.[1] carried out Hartree-Fock and Fenske-Hall calculations on the hypothetical complex $V_2(O_2CH)_4$ and concluded that this molecule, could it be synthesized, should exhibit a triple V-V bond and a short metal-metal distance of 2.0-2.1 Å. Still at the Hartree-Fock level of approximation, Lüthi and Bauschlicher (LB)[2] investigated investigated $(C_5H_5V)_2C_8H_8$ (**1**), a complex of the $(V_2)^{4+}$ dimetal unit, previously characterized by Elschenbroich et al.[7] LB appropriately noticed the involvement of the 3d orbitals in both the metal-metal and the metal-ligand bonding. However, their conclusions were quantitatively and even qualitatively in error because of the neglect of large correlation effects mainly originating in the dimetal unit. Later on, Mougenot, Demuynck, Bénard, and Bauschlicher (MDBB)[3] revisited this calculation and illustrated the importance of correlation by showing that the state of lowest energy found *at the Hartree-Fock level* is a quintet, in complete contradiction with the singlet ground state experimentally reported for this molecule.[8] Electron correlation of the metal d electrons was then introduced in the calculation of several states of different multiplicities ($^1A_1$, $^3B_1$, $^5A_1$). The correlation energy was computed through configuration interaction (CI) expansions, obtained by generating all configurations belonging to the proper spin multiplicity and symmetry out of an active space limited to 12 frontier orbitals. These orbitals were taken from the SCF MO set *optimized for the* $^5A_1$ state.[3] The CI calculations restored the singlet $^1A_1$ as the ground state, with a singlet-triplet (S-T) energy separation of ~3 kcal/mol. It appeared later that this S-T separation is in reasonable agreement with the experimental value of 5.5 kcal/mol.[8] The description of the metal-metal interaction in terms of a weak triple bond was later corroborated by the results of multiple-scattering Xα calculations,[4] in spite of differing estimate for the metal-metal bond order [1.1 for the CI calculation of MDBB, 2.6 for the MS-Xα calculation of Weber, Chermette, and Heck (WCH).[4]]. In view of the rather satisfactory results obtained for $(Cp\text{-}V)_2C_8H_8$, we used the same limited CI approach for a preliminary description of the bonding in the cyclopentadienyl butanediyl vanadium dimer, $(C_5H_5\text{-}V\text{-}C_4H_8)_2$ (**2**).[6]

As this work came to an end, we became conscious that both the choice of the starting set of MOs (those of the RHF quintet $^5A_1$ state) and the limitation of the active space of CI to a limited number of frontier MOs with high metal character favor the exclusive correlation of the metal d electrons, assumed to be quantitatively most important. This procedure could provide an unbalanced description of the metal-metal and metal-ligand interactions and could eventually bias the description of the electronic structure. This problem is not so important when the metal-metal coupling, on the one hand, the metal-ligand interactions, on the other hand, are effective through separate sets of d metal orbitals, such as in dimetal tetracarboxylate molecules or other "lantern-type" complexes.[9] As noticed by LB,[2] this is not the case for $(Cp\text{-}V)_2C_8H_8$ and related systems which exhibit, in contrast, considerable entanglement and even possible competition between the metal-metal and metal-ligand stabilizing interactions.

Our goal in the present work was to design, in the frame of the Hartree-Fock/CI methodology, an approach providing a balanced and reliable description of the metal-metal and metal-ligand interactions and a stable estimate of the S-T energy separation. This approach was then applied to compare the electronic structure and properties of four dimers of vanadium(I), -(II), and -(III), namely, μ-(η^5:η^5-cyclooctatetraene)-bis[(η^5-cyclopentadienyl)vanadium], $(C_5H_5\text{-}V)_2C_8H_8$ (**1**), bis[μ-(butanediyl)-(η^5-cyclopentadienyl)vanadium] $(C_5H_5\text{-}V\text{-}C_4H_8)_2$ (**2**), diindenyldivanadium $(C_9H_7\text{-}V)_2$ (**3**), and benzene bis[μ-(hydrido)-(η^5-cyclopentadienyl)vanadium] $(C_5H_5\text{-}V\text{-}H)_2C_6H_6$ (**4**) (Figure 1). No quantum chemical calculation had been previously reported for either **3** or **4**.

Computational Strategy

The strategy used by MDBB in their estimation of the nondynamic correlation in **1** was based upon the assumption that the major correlation effects originate in the frontier orbitals describing the direct metal-metal bonds. The RHF optimization of the $^5A_1$

(1) Cotton, F. A.; Diebold, M. P.; Shim, I. *Inorg. Chem.* **1985**, *24*, 1510.
(2) Lüthi, H. P.; Bauschlicher, C. W., Jr. *J. Am. Chem. Soc.* **1987**, *109*, 2046.
(3) Mougenot, P.; Demuynck, J.; Bénard, M.; Bauschlicher, C. W., Jr. *J. Am. Chem. Soc.* **1988**, *110*, 4503.
(4) Weber, J.; Chermette, H.; Heck, J. *Organometallics* **1989**, *8*, 2544.
(5) Arif, A. M.; Cowley, A. H.; Pakulski, M.; Norman, N. C.; Orpen, A. G. *Organometallics* **1987**, *6*, 189.
(6) Poumbga, C.; Daniel, C.; Bénard, M. *Inorg. Chem.* **1990**, *29*, 2387.
(7) Elschenbroich, Ch.; Heck, J.; Massa, W.; Schmidt, R. *Angew. Chem.* **1983**, *95*, 319. (b) Elschenbroich, Ch.; Heck, J.; Massa, W.; Nun, E.; Schmidt, R. *J. Am. Chem. Soc.* **1983**, *105*, 2905.
(8) Bachmann, B.; Hahn, F.; Heck, J.; Wünsch, M. *Organometallics* **1989**, *8*, 2523.
(9) See for instance: Davy, R. D.; Hall, M. B. *J. Am. Chem. Soc.* **1989**, *111*, 1268, and references cited therein.

0002-7863/91/1513-1090$02.50/0

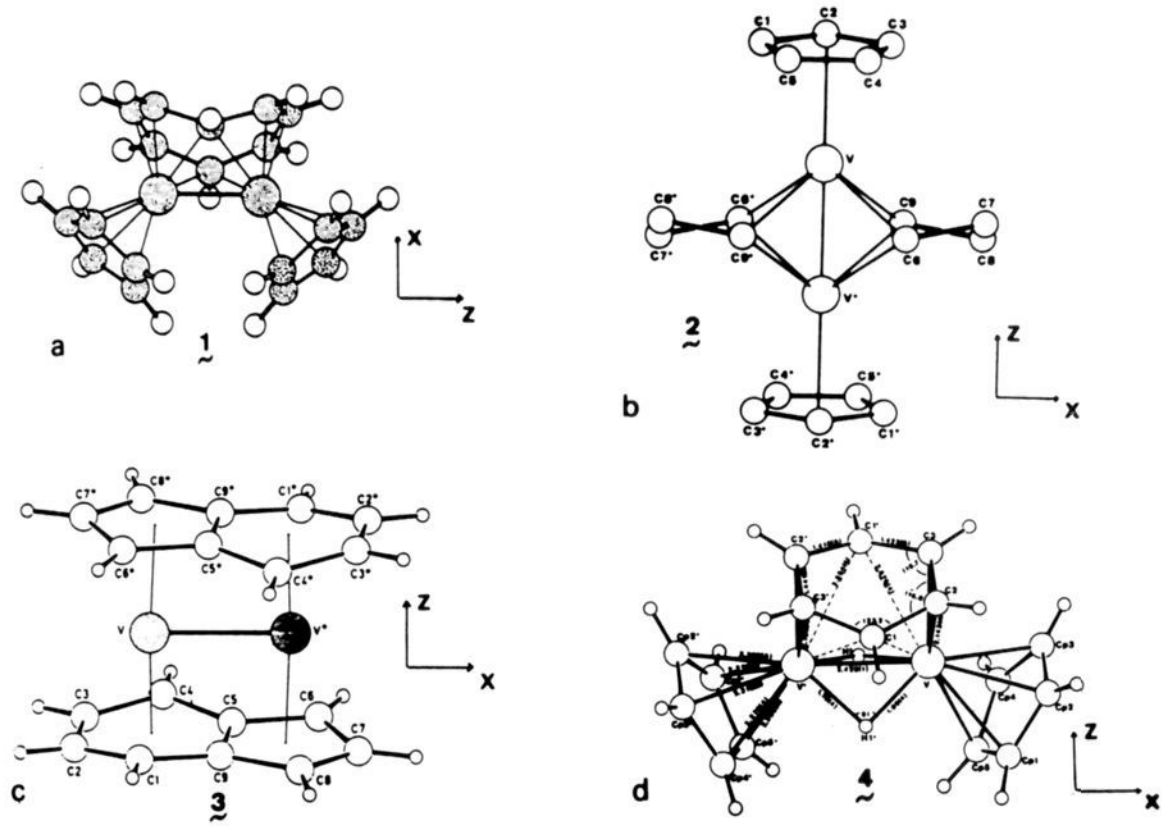

Figure 1. Representation of the four divanadium complexes: $(C_5H_5\text{-}V)_2C_8H_8$ (**1**), $(C_5H_5\text{-}V\text{-}C_4H_8)_2$ (**2**), $(C_9H_7\text{-}V)_2$ (**3**), $(C_5H_5\text{-}V\text{-}H)_2C_6H_6$ (**4**).

state of lowest energy localizes the four open-shell orbitals $(29a_1)^1$, $(30a_1)^1$, $(26b_1)^1$, and $(27b_1)^1$ on the dimetal subunit, with an efficiency comparable to that of a CASSCF[10] calculation carried out on the same active space. The most important part of the correlation energy for the states of lower spin multiplicity could then be retrieved from a small CI expansion carried out upon this set of four orbitals, augmented with the doubly occupied MO $17b_2$ describing the (metal–C_8H_8–metal) stabilizing interaction and with its metal–metal and metal–ligand antibonding counterparts. As stated in the introduction, in this approach somewhat arbitrarily separates the metal–metal coupling from the metal–ligand interactions and gives greater importance to the former without clear justification.

Since a CASSCF optimization accounting for both the metal–metal and the metal–ligand interactions is not technically possible at the present time, we decided to carry out multireference CI expansions starting from previously improved sets of occupied and virtual orbitals. The selection of the improved orbitals was carried out through preliminary single-reference CI expansions, using as a selection criterion the population of the natural orbitals (NOs) obtained by diagonalizing the one-electron density matrix.[11-13]

The first problem was to select the starting set of vectors that would undergo the improvement procedure. The RHF wave function of lowest energy, corresponding in all cases to a quintet state, was now ruled out since it already destroys the balance of the interactions to the benefit of the dimetal unit. The singlet wave function of lowest energy does not represent a better choice since it is biased toward an unrealistic configuration due to correlation artifacts.[2] The selection of a specific closed shell configuration, for example, the one corresponding to a triple bond in **1**, appears somewhat arbitrary and corresponds to a very high energy. It finally appeared to us that the best compromise could well correspond to the RHF wave function of the lowest triplet state. This wave function combines a proper description of the metal–ligand interactions with an adequate optimization of the HOMO/LUMO pair which appears from the $X\alpha$ calculations to be almost devoid of ligand character.[4] Starting from this orbital set, the process of orbital optimization was carried out by using a multistep procedure in the spirit of the iterative natural orbital method first introduced by Bender and Davidson.[14]

Step 1. Select the set of occupied orbitals accounting for either the metal–metal or the metal–ligand interactions, in practice, all occupied orbitals with a significant metal contribution. The corresponding electrons will be correlated by means of a single-reference CI generating all single and double excitations toward the valence part of the virtual space (SDCI expansion 1). The reference configuration is the ground-state singlet. The one-electron matrix is diagonalized, generating the NOs as eigenvectors and their occupation numbers as eigenvalues. Löwdin[11] has shown that most of the correlation energy should concentrate in the excitations toward the "virtual" (i.e., weakly occupied) NOs with largest occupation numbers. Conversely, these excitations should *originate* in the strongly occupied NOs with smallest occupation number. This latter statement provides a criterion for cutting the number of correlated electrons: strongly occupied NOs with occupation numbers above 1.99 e will not be retained for the next step.

It must be noted that the strongly occupied NOs are linear combinations of the occupied *and virtual* SCF orbitals. The occupied set of NOs therefore does not exactly reproduce the SCF energy of the lowest triplet. The mixing between the occupied

(10) Complete Active Space SCF: (a) Roos, B. O.; Taylor, P. M.; Siegbahn, P. E. M. *Chem. Phys.* **1980**, *48*, 157. (b) Siegbahn, P. E. M.; Almlöf, J.; Heiberg, A.; Roos, B. O. *J. Chem. Phys.* **1981**, *74*, 2384. (c) Roos, B. O. *Int. J. Quantum Chem.* **1980**, *S14*, 175.

(11) Löwdin, P. O. *Phys. Rev.* **1955**, *97*, 1474.

(12) Shavitt, I. In *Methods of Electronic Structure Theory*; Schaefer, H. F., III, Ed.; Plenum: New York, 1977; Section 8.3, pp 248–251, and references cited therein.

(13) Caballol, R.; Malrieu, J. P. *Chem. Phys.* **1990**, *140*, 7.

(14) (a) Bender, C. F.; Davidson, E. R. *J. Phys. Chem.* **1966**, 70, 2675. (b) Bender, C. F.; Davidson, E. R. *J. Chem. Phys.* **1967**, *47*, 4972. (c) Bender, C. F.; Davidson, E. R. *Phys. Rev.* **1969**, *183*, 23. (d) Schaefer, H. F., III *J. Chem. Phys.* **1971**, *54*, 2207.

Table I. Characteristics of the CI Expansions Carried out on Molecules $(Cp–V)_2C_8H_8$ (**1**), $(Cp–V–C_4H_8)_2$ (**2**), $(C_9H_7–V)_2$ (**3**), and $(Cp–V–H)_2C_6H_6$ (**4**)

	1		**2**		**3**		**4**	
	T[a]	S[b]	T[a]	S[b]	T[a]	S[b]	T[a]	S[b]
SCF energy	−0.3347[h]	−0.1441[h]	−1.0010[i]	−0.7613[i]	−0.1239[j]	−0.0120[j]	−0.7265[k]	−0.5597[k]
SDCI 1								
correlated electrons		22		26		18		20
MO space[c]		52		48		41		51
no. of CSFs[d]		25781		26283		10591		21404
energy, hartrees		−0.4642[h]		−1.0893[i]		−0.2220[j]		−0.8441[k]
SDCI 2								
correlated electrons		14		12		14		14
MO space[e]		177		188		171		173
no. of CSFs[d]		178042		150021		165628		169912
energy, hartrees		−0.4734[h]		−1.0955[i]		−0.2532[j]		−0.8790[k]
SDCI 3								
correlated electrons	14	14	12	12	14	14	14	14
MO space[f]	41	41	31	31	43	43	41	41
no. of CSFs	26683	7276	10272	2957	30006	8131	26769	7308
energy, hartrees	−0.5674[h]	−0.4722[h]	−1.1896[i]	−1.0939[i]	−0.3389[j]	−0.2619[j]	−0.9505[k]	−0.8693[k]
MRCI 4								
ref config		7		4	3	5	5	7
no. of CSFs		145798		17456	191533	86176	94763	106425
energy, hartrees		−0.6192[h]		−1.2185[i]	−0.3728[j]	−0.3758[j]	−0.9884[k]	−0.9851[k]
MRCI 5, final[g]								
ref config (RC)	6	9	4	5	5	7	8	10
no. of CSFs	221369	134605	25377	19825	228997	123015	260299	146876
coef for the leading term	0.7908	0.6587	0.8065	0.5946	0.8388	0.7123	0.8503	0.7405
coef for all RCs	0.9271	0.9215	0.9431	0.9429	0.9074	0.9078	0.9163	0.9299
total energy, h	−0.6233[h]	−0.6363[h]	−1.2229[i]	−1.2290[i]	−0.3759[j]	−0.3892[j]	−0.9968[k]	−1.0077[k]
S–T energy separation, cm^{-1}	2820		1320		2890		2380	
total energy, h (with Davidson's correction)	−0.6524[h]	−0.6689[h]	−1.2382[i]	−1.2445[i]	−0.4195[j]	−0.4333[j]	−1.0361[k]	−1.0392[k]
S–T energy separation, cm^{-1}	3580		1380		3000		680	

[a] Lowest triplet. [b] Leading configuration of the ground state. [c] Taken from SCF wave function of the lowest triplet. [d] Number of configuration state functions really involved in the CI expansion (accounting for the restriction of the CSF space to the first-order interacting space). [e] Strongly occupied NOs from SDCI 1 with occupation number <1.99, augmented from the complete virtual space. [f] All occupied NOs from SDCI 2 with occupation number $>10^{-4}$; same number of correlated electrons as in SDCI 2. [g] Same MO space and number of correlated electrons as in SDCI 3. In all cases, the space of reference configurations for the singlet state contains the following configuration state functions (CSFs): $\sigma^2\delta^2\delta^{*0}\sigma^{*0}$, $\sigma^2\delta^0\delta^{*2}\sigma^{*0}$, $\sigma^0\delta^2\delta^{*0}\sigma^{*2}$, $\sigma^0\delta^0\delta^{*2}\sigma^{*2}$, $\sigma^1\delta^1\delta^{*1}\sigma^{*1}$. The presence of these five configurations in the reference space ensures a correct dissociation of the σ and δ bonds. There are four corresponding configurations for the triplet state, namely, $\sigma^2\delta^1\delta^{*1}\sigma^{*0}$, $\sigma^0\delta^1\delta^{*1}\sigma^{*2}$, $\sigma^1\delta^2\delta^{*0}\sigma^{*1}$, $\sigma^1\delta^0\delta^{*2}\sigma^{*1}$. Other CSFs involving the π^* orbital are added to the reference space if they contribute to the balance between the reference spaces respectively associated with the singlet and with the triplet states and if they show up in the list of the most important configurations. For molecule **4**, the additional reference configurations are as follows: $\sigma^2\delta^2\pi^0\pi^{*2}$, $\sigma^2\delta^{*2}\pi^0\pi^{*2}$, $\sigma^2\delta^1\delta^{*1}\pi^1\pi^{*1}$, $\sigma^1\sigma^{*1},\delta^2\pi^1\pi^{*1}$, $\sigma^1\sigma^{*1}\delta^{*2}\pi^1\pi^{*1}$ for the singlet state and $\sigma^2\delta^1\delta^{*1}\pi^0\pi^{*2}$, $\sigma^2\delta^2\delta^{*0}\pi^1\pi^{*1}$, $\sigma^2\delta^0\delta^{*2}\pi^1\pi^{*1}$, $\sigma^1\sigma^{*1}\delta^1\delta^{*1}\pi^1\pi^{*1}$ for the triplet. [h] Shifted by 2573 hartrees. Lowest SCF energy ($^5A_1$ state): −2573.4619 hartrees. [i] Shifted by 2577 hartrees. Lowest SCF energy (^5A_g state): −2578.1296 hartrees. [j] Shifted by 2571 hartrees. Lowest SCF energy (^5A_g state): −2571.1880 hartrees. [k] Shifted by 2497 hartrees. Lowest SCF energy ($^5A_1$ state): −2497.8006 hartrees.

and the virtual set is generally regarded as an artifact and corrected by generating *approximate* NOs obtained from separate diagonalizations of the density matrix restricted either to the subspace of the occupied or to the subspace of the virtual SCF MOs.[15] This correction was *not* carried out in the present case for the following reason: it was noticed that the SCF energy of the lowest triplet computed with the final set of NOs is effectively increased by about 0.01 hartree, *but at the same time, the energy of the configuration with major weight in the description of the singlet ground state is improved by a similar amount.* Since we are interested in the singlet–triplet energy separation, the exact NOs provide a starting point that is not connected any longer in a preferential way to either of these two states.[16]

Step 2. The electrons associated with the selected strongly occupied NOs are submitted once again to a single-reference SDCI treatment now involving the complete set of virtual orbitals (i.e., the set of weakly occupied NOs generated in step 1, *completed by the set of SCF canonical frozen virtuals*). This represents SDCI expansion 2. Natural orbitals are derived, and a subset of *virtual* NOs is now selected according to the occupation criterion. All NOs with occupation numbers lower than 10^{-4} e are deleted. The remaining NOs represent the final set of optimized orbitals to be used in the next multireference CI steps. Although the number of virtual orbitals is drastically reduced, the energy obtained from a single-reference SDCI carried out on the final set (SDCI expansion 3) is extremely close to the energy obtained with the complete basis of virtual orbitals (Table I).

Step 3. The final set of optimized NOs is used to carry out a multireference CI (MRCI expansion 4) for both the ground-state singlet and the lowest triplet states. All configurations having coefficients[17] larger than 0.1 in SDCI 3 are taken as references.

Step 4. The switch to multireference modifies the CI coefficients. The number of reference configurations to be considered in the CI expansions describing the singlet and triplet states must generally be increased. Moreover, the stability of the computed S–T energy separation requires the sets of reference configurations to be equivalent for both states. An additional step (MRCI expansion 5, final) is therefore needed to obtain consistent and stable results.

(15) (a) Barr, T. L.; Davidson, E. R. *Phys. Rev. A* **1970**, *1*, 64. (b) Reinhardt, W. P.; Doll, J. D. *J. Chem. Phys.* **1969**, *50*, 2767. (c) Hay, P. J. *J. Chem. Phys.* **1973**, *59*, 2468. (d) Karlström, G.; Jönsson, B.; Roos, B. O.; Siegbahn, P. E. M. *Theor. Chim. Acta* **1978**, *48*, 59. (e) Jorgen, H.; Jensen, A.; Jorgensen, P.; Ågren, H.; Olsen, J. *J. Chem. Phys.* **1988**, *88*, 3834. (f) Illas, F.; Rubio, J.; Ricart, J. M. *J. Chem. Phys.* **1988**, *89*, 6376. (g) Roos, B. O.; Siegbahn, P. E. M. In *Methods of Electronic Structure Theory*; Schaefer, H. F., III, Ed.; Plenum: New York, 1977; Section 2.4, pp 288–291, and references cited therein.

(16) Another approach to the problem of determining NOs for simultaneous calculations on several electronic states consists of the determination of *average natural orbitals* obtained by diagonalizing the average of the first-order density matrices of the states of interest. See for instance: Houlden, S. A.; Czismadia, I. G. *Theor. Chim. Acta* **1973**, *30*, 209.

(17) Possibly determined from the accumulated contributions of all relevant configuration state functions.

Table I summarizes the characteristics of the five CI expansions carried out for systems **1–4**. The coefficient accounting for the accumulated contributions of all reference states in the final expansions (singlet or triplet) is higher than 0.9 for all molecules. With one exception (molecule **4**), these coefficients are remarkably close for the ground-state singlet and for the lowest triplet of the same molecule, indicating that the level of approximation is quite similar for both states. The final energy values reported in Table I include Davidson's correction to the energy, which provides an estimate of the effect of quadruple excitations with respect to the reference states.

Computational Details

The molecular geometries used for the calculations were taken from the experimental determinations of Elschenbroich et al.[7] for **1** and of Jonas et al. for **2**,[18] **3**,[19] and **4**.[20] These geometries were slightly modelized to retain a perfect C_{2h} symmetry for **2** and **3**, and a C_{2v} symmetry for **1** and **4** (Figure 1). The basis set for vanadium was the (13,7,6) set optimized by Hyla-Kryspin et al.[21] and incremented with one *p* function of exponent 0.15. It was contracted into [5,3,3], which is minimal for the inner shells and for the 4p shell, double ζ for 4s, and triple ζ for the 3d shell. Basis sets of respective sizes (9,5)[22] and (4)[22] were used for carbon and hydrogen, except for the hydrido H atoms, and contracted to split valence. For the hydrido atoms, a (6,1) basis set was obtained by adding a *p*-type polarization function of exponent 0.8 to the (6s) basis set reported by Huzinaga.[23] This basis set was contracted into (3,1). The SCF calculations and 4-index transformations were carried out by using the ASTERIX system of programs,[24] whereas the configuration interaction expansions were performed by using Siegbahn's contracted CI program.[25]

Electronic Structure of the Divanadium Complexes

1. $(C_5H_5–V)_2C_8H_8$ (1). The electronic structure of the singlet ground state deduced from the final CI calculation (MRCI 5) is in agreement with the previous results from MDBB[3] and WCH.[4] Each vanadium atom is formally populated with three electrons, giving rise to a triple metal–metal bond. As pointed out in former studies,[2–4] the π, σ, and δ components of the metal–metal bonds are mixed in all representations, so that the metal orbitals cannot be attributed a definite character. This is especially true for the two highest orbitals of representation A_1, referred to as $29a_1$ and $30a_1$.[26]

The natural orbitals of the final CI calculation with major metal character should be analyzed as pairs of bonding/antibonding orbitals, with a total population very close to two electrons. The distribution of the population between the bonding and the antibonding NOs scales the more or less delocalized character of the electron pair described by this subset of two complementary orbitals. Ending up with nearly equal populations for both the bonding and the antibonding NOs means that the electron pair is almost completely relocalized in separate moieties of the system, leading to a molecule with diradical character. In contrast, a population close to zero for the antibonding NO would be the sign of a quasi-complete delocalization of the electron pair.

The natural orbital populations are displayed in Table II. The density generated by the HOMO/LUMO pair ($30a_1/26b_1$) is represented in the plane containing the V–V axis and perpendicular to the cycles (Figure 2a,b). The tilt of the HOMO lobes in the *x*Oz plane (Figure 2a) reflects the mixing between π and δ (9.5% σ, 29% π, 57% δ, and 4% ligand characters) leading to a V–V bond strongly bent toward the cyclooctatetraene ring. Note that this bent metal orbital looks quite similar to the one displayed by WCH.[27] At variance from the Xα results, however, the CI description of the electron pair also involves the antibonding counterpart of $30a_1$, natural orbital $26b_1$ (Figure 2b). The respective populations of $30a_1$ and $26b_1$ are 1.28 and 0.71 e (Table II), corresponding to a large relocalization. The weakness of this bond is an obvious consequence of the dominant δ character of the HOMO/LUMO pair. In the MS-Xα calculation, the weakness of the δ metal–metal bond appears no more than virtually and should be inferred from the small energy gap between the HOMO and the LUMO.[4] As for one-determinant SCF wave functions, the space of occupied Xα orbitals does not account for the electron relocalization that arises in the case of weak or vanishing overlap. This should explain why the V–V bond order computed from MS-Xα appears so much higher (2.6)[4] than the bond orders obtained by using the CI formalism either in the study of MDBB (1.1)[3] or in the present work (1.5).

Another pair of bonding/antibonding orbitals in the same representations ($29a_1/27b_1$) displays almost exclusive metal character (92%). Most of the metal character (57% of the electron density) comes from the contribution of the σ orbitals and 31% from the π orbitals. The density distribution associated with $29a_1$ (Figure 2c) presents a saddle point in between the two metals, and the bond appears slightly bent *away* from the C_8H_8 cycle. The density value at the saddle point is about 4 times higher than for orbital $30a_1$, illustrating the difference in overlap and bond strength. The respective populations of $29a_1$ and $27b_1$ are 1.65 and 0.34 e, reflecting the description of this orbital pair in terms of a direct σ/π bond, stronger than the δ coupling, but still significantly affected by relocalization. The description of this orbital pair has been modified with respect to the previous work of MDBB, who attributed it a dominant π/π^* character with respective occupations of 1.28 and 0.70 e.[3] This modification should be ascribed to the better orbital optimization carried out in the present work through successive CI expansions. The presence of a second electron pair strongly localized on the dimetal subunit is also at variance from the MS-Xα results of WCH reporting for all frontier orbitals (except for the HOMO/LUMO pair) a considerable delocalization over the whole complex.

The last pair of orbitals with major metal character corresponds to natural orbitals $17b_2/15a_2$. At variance from the former metal orbitals, this electron pair is largely delocalized over six carbon

Table II. $(C_5H_5–V)_2C_8H_8$ (**1**): Population of the Natural Orbitals Obtained for the Lowest Singlet and Triplet States and Distribution of This Population among the Molecular Fragments (from the Mulliken Population Analysis of the Singlet Ground-State NOs)

	orbital popul, e (singlet)	metal, %	C_8H_8, %	Cp, %	orbital popul, e (triplet)
b_1 (π_{Cp})	1.98	16	6	78	1.98
b_2 (π_{Cp})	1.98	21	17	62	1.98
a_1	1.97	26	42	32	1.97
a_2 ($\pi_{C_8H_8}/\delta^*_{V_2}$)	1.92[a]	34	64	2	1.94
b_2 ($\pi/\delta)_{V_2}$	1.86	61	37	2	1.88
a_1 ($\sigma/\pi)_{V_2}$	1.65	93	4	3	1.61
a_1 ($\delta/\pi)_{V_2}$	1.28	96	2	2	1.03
b_1 ($\delta^*/\pi^*)_{V_2}$	0.71	98	1	1	0.96
b_1 ($\sigma^*/\pi^*)_{V_2}$	0.34	92	2	6	0.37
a_2 ($\pi^*/\delta^*)_{V_2}$	0.13	73	26	12	0.11
b_2	0.06	48	51	16	0.05

[a] Brackets are connecting pairs of bonding/antibonding NOs defined on the same atomic orbitals. The sum of their orbital populations is approximately two electrons.

(18) Jonas, K.; Rüsseler, W.; Krüger, C.; Raabe, E. *Angew. Chem., Int. Ed. Engl.* **1986**, *25*, 925.
(19) Jonas, K.; Rüsseler, W.; Krüger, C.; Raabe, E. *Angew. Chem., Int. Ed. Engl.* **1986**, *25*, 928.
(20) Jonas, K.; Wiskamp, V.; Tsay, Y. H.; Krüger, C. *J. Am. Chem. Soc.* **1983**, *105*, 5480.
(21) Hyla-Kryspin, I.; Demuynck, J.; Strich, A.; Bénard, M. *J. Chem. Phys.* **1981**, *75*, 3954.
(22) Huzinaga, S. Technical Report, University of Alberta, Edmonton, 1971.
(23) Huzinaga, S. *J. Chem. Phys.* **1965**, *42*, 1293.
(24) (a) Ernenwein, R.; Rohmer, M.-M.; Bénard, M. *Comp. Phys. Commun.* **1990**, *58*, 305. (b) Rohmer, M.-M.; Demuynck, J.; Bénard, M.; Wiest, R.; Bachmann, C.; Henriet, C.; Ernenwein, R. *Comp. Phys. Commun.* **1990**, *60*, 127. (c) Wiest, R.; Demuynck, J.; Bénard, M.; Rohmer, M.-M.; Ernenwein, R. *Comp. Phys. Commun.* **1990**, in press.
(25) Siegbahn, P. E. M. *Int. J. Quantum Chem.* **1983**, *23*, 1869.
(26) The orbital numbering adopted by LB and MDBB and used in the present work accounts for both core and valence orbitals. The numbering restricted to valence MOs, used by WCH, leads to the following labels for the HOMOs in each representation: $19a_1$, $10a_2$, $15b_1$, $12b_2$.
(27) See Figure 3 of ref 4. In the notation system used by WCH, the HOMO contour plot is referred to as $19a_1$, displayed in the *y*Oz plane.

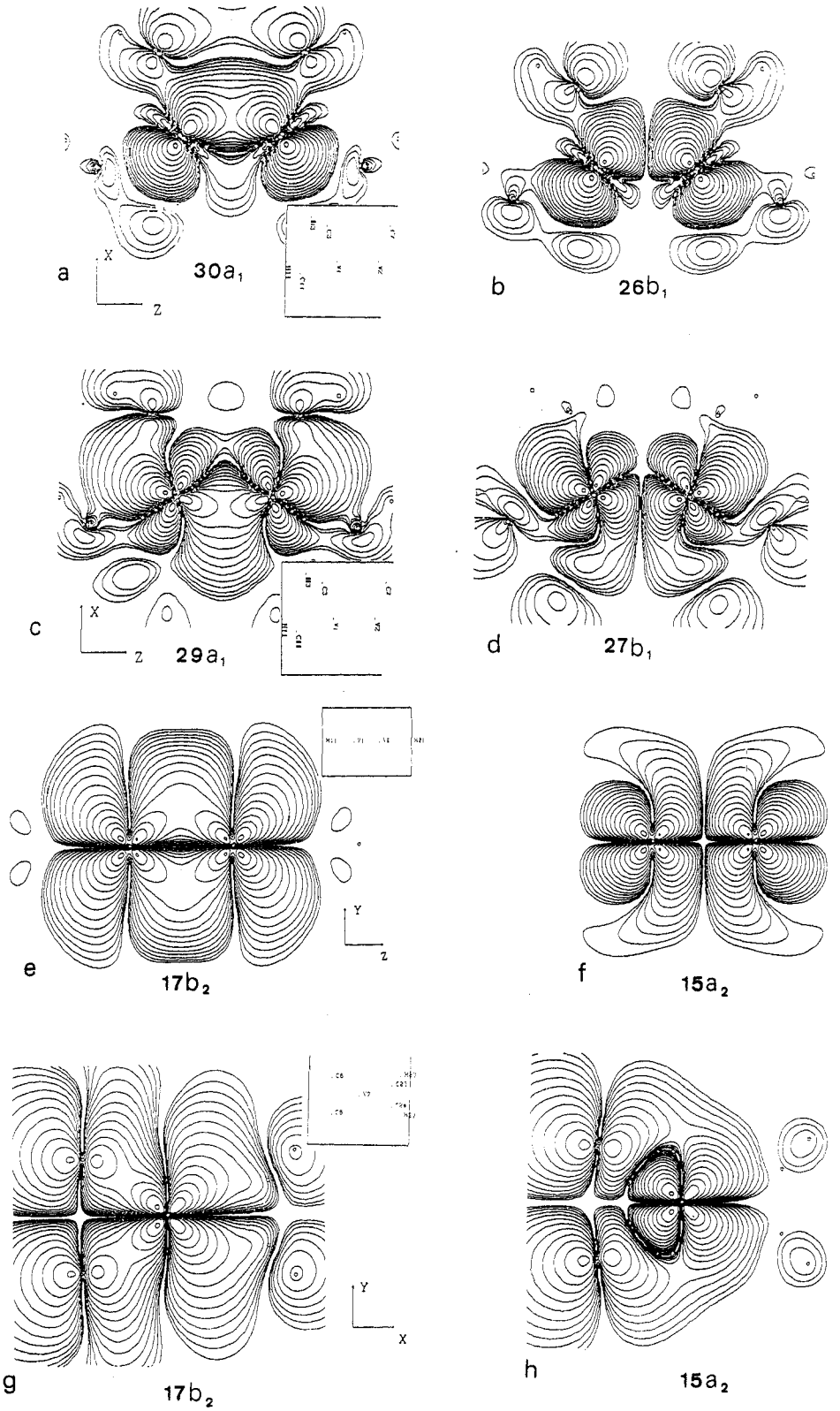

Figure 2. Plot of the electron densities associated with some natural orbitals obtained for $(C_5H_5\text{-}V)_2C_8H_8$: (a) orbital $30a_1$ (occupation 1.28 e); (b) orbital $26b_1$ (occupation 0.71 e); (c) orbital $29a_1$ (occupation 1.65 e); (d) orbital $27b_1$ (occupation 0.34 e). Plane xOz, containing the two vanadium atoms and perpendicular to the cycles: (e) orbital $17b_2$ (occupation 1.86 e); (f) orbital $15a_2$ (occupation 0.13 e). Plane yOz, containing the two vanadium atoms and parallel to the average cycle plane: (g) orbital $17b_2$; (h) orbital $15a_2$. Plane coplanar to xOy, containing one vanadium atom and perpendicular to the V–V axis. The density in two successive contours differs by a factor of 2.

atoms of the C_8H_8 cycle (the two C_8H_8 carbons lying in the xOz plane have no π contribution because of symmetry). The metal weight in orbital $17b_2$ is 61% only (72% for the antibonding counterpart $15a_2$). This delocalization is the consequence of a double interaction reported in the extended Hückel interaction diagram of Figure 3.

On the one hand, a low-lying orbital of the $(V\text{–}Cp)_2^{2+}$ fragment with metal–metal π bonding character interacts with the LUMO of the $C_8H_8^{2-}$ moiety. On the other hand, a doubly occupied, π bonding orbital of $C_8H_8^{2-}$ interacts with a high-lying δ bonding orbital of the dimetal fragment (Figure 3). Natural orbital $17b_2$ can be interpreted as a mixture of the orbitals resulting from both

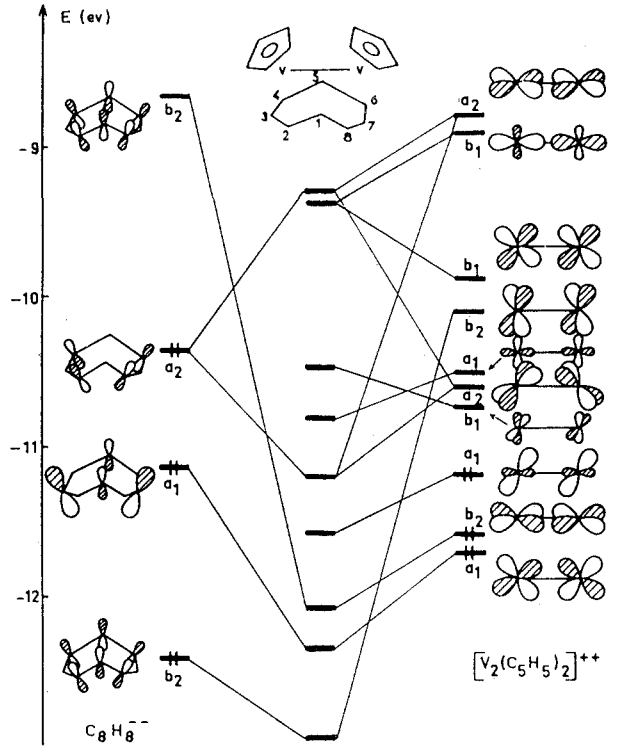

Figure 3. Orbital interaction diagram between the $[V_2(C_5H_5)_2]^{2+}$ and the $(C_8H_8)^{2-}$ fragments leading to molecule **1** (from extended Hückel calculations).

interactions. It combines a dominating V–V π character (40%) with a nonnegligible δ contribution (21%), the remaining contribution coming almost completely (37%) from the C_8H_8 cycle. Parts e and g of Figure 2 illustrate the respective metal–metal and metal–ligand bonding characters of $17b_2$ by displaying the orbital density in the planes (i) containing the V–V line and parallel to the average C_8H_8 plane (yOz, Figure 2e) and (ii) perpendicular to the V–V line through one vanadium atom and containing two carbon atoms of C_8H_8 (Figure 2g). Parts f and h of Figure 2 represent in the same planes the density of the weakly occupied counterpart $15a_2$ of $17b_2$, which is both metal–metal and metal–ligand antibonding. In spite of its delocalization over the cyclooctatetraene moiety, this electron pair accounts for a large part of the overall metal–metal bonding character. As a matter of fact, the respective occupations of $17b_2$ and $15a_2$ are 1.86 and 0.13 e, which means that the correlation effects involving these orbitals are relatively minor compared to those developing between the combinations of metal orbitals left unaffected by strong interactions with the ligands. In the present case, interaction with C_8H_8 enhances the energy gap between the V–V bonding and antibonding combinations, thus drastically reducing the contribution of this latter component to the correlated wave functions.

To achieve the display of the most important contributions to the metal–metal interactions, it is worth mentioning orbital $14a_2$, a predominantly ligand orbital which results from the interaction of the HOMO of $C_8H_8^{2-}$, a nonbonding π orbital with major weight on the four equivalent carbons of the cycle, with a V–V antibonding orbital displaying mixed π^* and δ^* character (Figure 3). This natural orbital, with a population of 1.92 e and a metal weight of 34%, corresponds to orbital $10a_2$ of WCH.

2. $(C_5H_5$–V–$C_4H_8)_2$ (2). Preliminary ab initio CI calculations on **2** have been recently reported, and the electronic structure of this complex has been discussed.[6] More detailed information can be gained from the interaction diagram of Figure 4. Each terminal carbon of the butanediyl ligands gives rise to a hybrid orbital oriented opposite to the tripod of the C–C and C–H bonds. These hybrids combine into four ligand orbitals belonging to different irreducible representations of the C_{2h} point group.

Each ligand orbital combination interacts with a divanadium orbital displaying metal–metal bonding character, thus giving rise

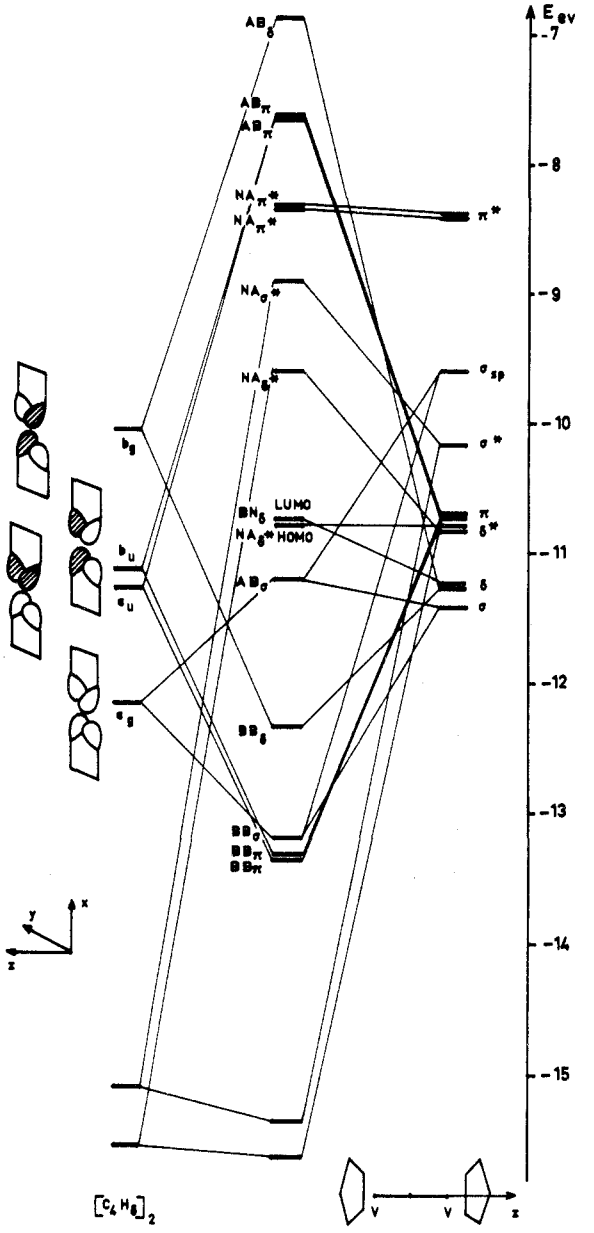

Figure 4. Orbital interaction diagram between the $[V_2(C_5H_5)_2]^{4+}$ and the $(C_4H_8)_2^{4-}$ fragments leading to molecule **2** (from extended Hückel calculations).

to four low-lying, delocalized orbitals with major weight on the butanediyl ligands, but characterized by some V–V bonding contribution. These four orbitals are labeled BB_π, BB_σ, and BB_δ, the first capital referring to the *vanadium–butanediyl* bonding character and the second capital to the *metal–metal* bonding character. They are displayed in Figure 5. These interactions are quite different in strength. The strongest ones are those involving the metal π orbitals (representations a_u and b_u), resulting in a stabilization of the ligand orbitals by more than 2 eV. Then comes the interaction of the δ metal orbital (d_{xy}) with the C_4H_8 combination of b_g symmetry, relatively high in energy because of the ligand–ligand repulsive interactions (Figure 4). In spite of the lateral overlap between the metal orbitals and the ligand ones (made more efficient, however, by the twisting of the butanediyl ions), the metal contribution to the resulting MO is quite large (38%, Table III) and the stabilization reaches 1 eV with respect to the δ level. The stabilization energy of the totally symmetric ligand combination reaches the same order of magnitude, but the origin of this stabilization is slightly more complex. The contribution of the lowest σ orbital of the $(Cp–V)_2$ fragment, an in-phase combination of the metal d_{z^2} orbitals, is not sufficient to explain the stabilization of the ligand combination. The key

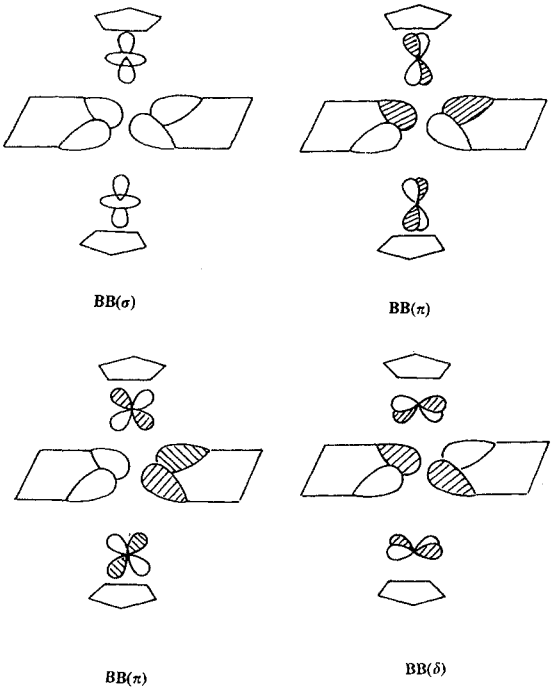

Figure 5. Scheme of the four combinations of the $(C_4H_8)_2$ lone pairs stabilized through interactions with metal–metal bonding orbital combinations. The orbital contributions from the Cp rings are omitted for clarity.

Table III. $(C_5H_5\text{–}V\text{–}C_4H_8)_2$ (2): Population of the Natural Orbitals Obtained for the Lowest Singlet and Triplet States and Distribution of This Population among the Molecular Fragments (from the Mulliken Population Analysis of the Singlet Ground-State NOs)

	orbital popul, e (singlet)	metal, %	C_4H_8, %	Cp, %	orbital popul, e (triplet)
BB_π (a_u)	1.97	36	35	29	1.97
BB_π (b_u)	1.97	35	36	29	1.97
BB_σ (a_g)	2.00	10	86	4	2.00
BB_δ (b_g)[a]	1.95	38	61	1	1.93
AB_σ (a_g)	1.59	93	2	5	1.61
NB_δ (a_g)	1.04	98	1	1	1.00
NA_{δ^*} (b_u)	0.95	99	0	1	0.99
NA_{σ^*} (b_u)	0.40	85	13	2	0.38
NA_{δ^*} (a_u)	0.04	84	15	1	0.05
NA_{π^*} (a_g)	0.02	88	2	10	0.02
NA_{π^*} (b_g)	0.01	82	13	5	0.01
AB_π (a_u)	0.01	73	19	8	0.01
AB_π (b_u)	0.01	72	17	11	0.02
AB_δ (b_g)	0.02	77	22	1	0.02

[a] Pairs of bonding/antibonding NOs defined as in Table II.

to the stabilization of the ligand orbital of a_g symmetry is another σ bonding orbital of the vanadium dimer, higher in energy by ~1.5 eV and constructed from sp hybrids (Figure 4). Interaction with this orbital instills significant sp character in both the stabilized BB_σ orbital and the AB_σ combination, thus almost completely preventing any destabilization of this orbital (Figure 4).

Extended Hückel calculations assign the HOMO and the LUMO to be quasi-degenerate, which is remarkably consistent with the natural orbital analysis of the ab initio CI wave function (Table III). The frontier orbitals are the metal–metal bonding and antibonding combinations of the metal $d_{x^2-y^2}$ (δ) orbitals. In the $(Cp\text{–}V)_2$ dimer, these orbitals are separated by ~0.5 eV, a gap in agreement with the small δ overlap. Neither δ nor δ^* can interact with the combination of ligand hybrids with appropriate symmetry. The energy gap is, however, offset in **2** due to a slight destabilizing interaction with ligand orbitals deeper in energy.

The conformation of the butanediyl dimer practically prevents any possibility of interaction between the ligand hybrids and any of the metal orbitals with V–V *antibonding* character. These interactions would be strictly symmetry-forbidden would the molecule belong to the D_{2h} symmetry point group. The Cp rings and, more important, the twisting of the C_4H_8 ligands break this symmetry into C_{2h}, but in the first approximation, the out-of-phase metal–metal orbital combinations remain nonbonding with respect to all combinations of ligand hybrids. As a consequence, one δ^* (d_{xy}-) and the two π^* orbitals, respectively referred to as NA_{δ^*} and NA_{π^*} remain practically unmodified with respect to their description and their energy in the $(Cp\text{–}V)_2$ fragment. The two last V–V antibonding orbitals, NA_{δ^*} and NA_{σ^*}, both of b_u symmetry, are destabilized because of interactions with ligand low-lying orbitals of the same symmetry (Figure 4). These orbitals describe the CH bonds of the butanediyl terminal carbons, and the interactions take place because of the short V···H contacts (2.10 and 2.57 Å) induced by the geometry of the butanediyl ligands.

A rather unusual consequence of the metal–ligand interactions is the rejection of all metal–metal bonding orbitals, except for the σ one, *above* the corresponding metal–metal *antibonding* orbitals (Figure 4).

The orbital diagram of Figure 4 helps in understanding the nature of orbital interactions at work in the present molecule, but leads to puzzling questions concerning the nature of the ground state. Since the butanediyl must be formally considered as $(C_4H_8)^{2-}$, the metal is V(III) and the number of valence electrons involved in the interactions between $(V_2)^{6+}$ and $(C_4H_8)_2{}^{4-}$ is 12. The four stabilized orbitals of the BB (bonding–bonding) type accommodate eight electrons. The problem is how the four extra electrons are distributed among the remaining frontier orbitals, since these orbitals are close in energy and subject to important localization effects because of their very high metal character. Table III displays the natural orbital analysis of the singlet ground state and lowest triplet configurations, as obtained from the final CI expansions. At variance from the other complexes of divanadium investigated in the present study, the populations of the δ and δ^* orbitals are remarkably close to 1 in the covalent singlet ground state. This is equivalent to considering the dimetal unit as a diradical, in agreement with the near degeneracy of the same orbitals at the extended Hückel level. Note, however, that the population of the δ NO remains slightly higher than that of δ^* (1.04 vs 0.95 e) in contradiction with the ordering of EH orbitals.

The localized character of the $d_{x^2-y^2}$ electrons was already noticed in the preliminary CI calculations carried out on the same molecule with an orbital space composed of the semioccupied MOs of the SCF quintet state of lowest energy, namely AB_σ, NB_δ, NA_{δ^*}, and NA_{σ^*}.[6] An effort had been made at that time to improve the energy and the description obtained from the CI expansion restricted to all excitations occurring in that small subset of four orbitals. The electrons of the BB_σ and BB_δ orbitals were added, and all single and double excitations with respect to the five important configurations of the small CI were considered toward the complete virtual space.[28] In spite of the large number of configurations, little energetical improvement was obtained with respect to the small four electrons/four MOs expansion (−2578.15926 compared to −2578.14651 hartrees). The procedure of selection and improvement of the active orbitals proposed in the present work has led to better results, since the energy was lowered to −2578.22898 hartrees by correlating 12 electrons.

3. Diindenyldivanadium (3). Molecule **3** has been synthesized and characterized by Jonas et al.[19] It looks like a dimetal sandwich complex, in which the two vanadium atoms are at a distance compatible with a multiple metal–metal bond (2.351 Å). The molecule has a center of inversion and belongs to the C_{2h} symmetry point group, so that each V atom is facing a five-membered ring and a six-membered ring (Figure 1c). Such a dinuclear sandwich structure seems to be extremely unusual. A similar structure has been proposed, but not confirmed, for complexes of dinickel and dicobalt with two pentalene molecules.[29]

(28) The same five reference configurations were selected in the present work (Table I).

(29) (a) Katz, T. J.; Acton, N. *J. Am. Chem. Soc.* **1972**, *94*, 3281. (b) Katz, T. J.; Acton, N.; McGinnis, J. *Ibid.* **1972**, *94*, 6205.

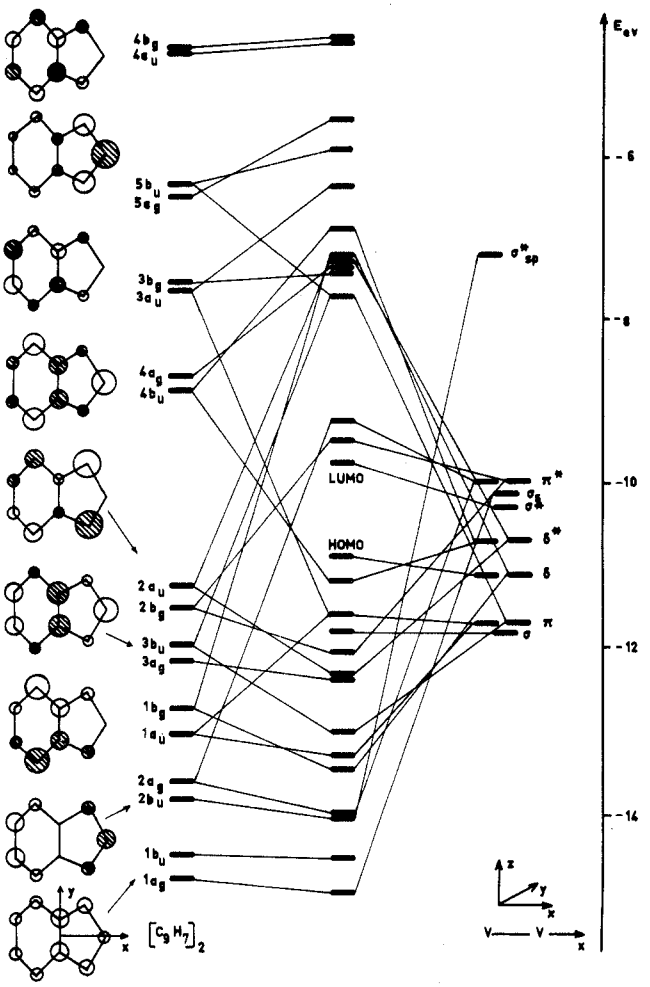

Figure 6. Orbital interaction diagram between the V_2^{2+} and the $(C_9H_7)_2^{2-}$ fragments leading to molecule **3** (from extended Hückel calculations).

Formally, the ligands are indenyl ions $(C_9H_7)^-$ so that the metal should be considered V(I), with four d electrons. This complex has therefore 2 electrons more than in the d^6 systems, such as **1**, that give rise to a formal triple V–V bond. Assuming the orbital ordering to remain similar, an electron pair should be therefore accommodated on a metal–metal antibonding orbital, either σ^* or δ^* (π^* orbitals are destabilized by metal–ligand interactions). As will be seen below, conclusions obtained from extended Hückel and ab initio CI calculations are divergent as far as this point is concerned.

Burdett and Canadell[30] have investigated the electronic structure of hypothetic di- and polymetallic sandwich compounds through extended Hückel calculations. Interaction diagrams are provided for sandwich naphthalene and pentalene metal dimers.[30] Although some basic assessments obtained from those diagrams remain valid, the asymmetric structure of the indenyl ion makes the interactions somewhat different. An interaction diagram specific to the $(V–C_9H_7)_2$ molecule is therefore displayed in Figure 6. As for the molecules investigated in ref 30, the most important interactions occur through the π orbitals of the indenyl ions, even though contributions from the σ orbitals are incidentally observed. The diagram has therefore been restricted to the (d metal)–(π ligand) interactions.

The indene molecule has nine π levels, five of which are occupied (all doubly occupied in the anion). These levels are split in the indene dimer, but the orbital combinations are never exactly in phase or out of phase due to the C_{2h} conformation of the dimer. As a consequence, the splitting is weak and becomes close to zero for high-energy, multinodal levels. The splitting of the vanadium d levels is much larger, as a consequence of the short metal–metal distance. The metal energy levels are lying between 10 and 12 eV, that is, in position to efficiently interact with both the occupied and the unoccupied levels of the indene dimer (Figure 6). One should also notice the presence of the relatively low lying σ combination of metal 4s orbitals and of its antibonding counterpart, which take part in weak stabilizing interactions with the low-lying indene π orbital combinations of appropriate symmetry (respectively a_g and b_u).

Burdett and Canadell (BC) have noticed that the δ and δ^* metal orbitals, corresponding to the d_{z^2} combinations (z is perpendicular to the indene planes), cannot give significant interactions with the naphthalene π orbitals of appropriate symmetry because the conical nodal surface of the d_{z^2} orbital points directly toward the π system of the cycles.[30] This remark does not hold so strictly in the present case because of the smaller size of the five-membered cycle. An interaction indeed occurs between the LUMO of the indene dimer, I, and the δ^* orbital of b_u symmetry, stabilizing

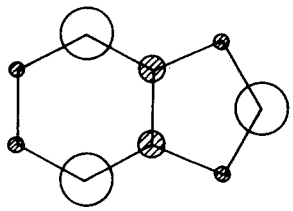

I

the latter one. A crossing occurs between the δ^* and δ levels, and the latter one, slightly destabilized, becomes the HOMO (Figure 6). The three other high-lying d metal levels are slightly destabilized through interactions with occupied ligand orbitals. The LUMO corresponds to the σ^* level, with a relatively large HOMO/LUMO gap of 1.1 eV. Note, however, that this gap is not influenced by the metal–ligand interaction but exclusively reflects the splitting of metal levels. The four highest occupied levels accommodate the eight metal d electrons, and, apart from the δ^* level discussed above, they are no more than slightly perturbed in energy by metal–ligand interactions. By decreasing order of energy, these levels are (i) the δ and δ^* orbitals of respective symmetry a_g and b_u; (ii) the π bonding orbital (d_{xy}-) of a_u symmetry, located in the plane parallel to the ligand cycles and subjected to both stabilizing and destabilizing interactions with the ligands, so that its energy remains unmodified; and finally (iii) the σ bonding orbital (symmetry a_g). The ground-state configuration deduced from EH is therefore $\sigma^2\pi^2\delta^2\delta^{*2}$. Below these frontier orbitals, 10 levels are found, corresponding to the π occupied levels of the indene dimer (the intercalated σ levels are not displayed), all stabilized to various degrees through interactions with the dimetal orbitals. Two interactions seem to be of special importance. One of them involves the highest occupied orbital of the indene dimer, II, well behaved for a large

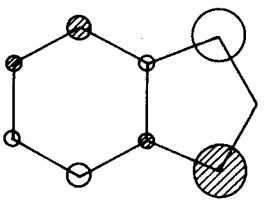

II

bonding overlap with the δ^* orbital of a_u symmetry, (d_{yz}-). The in-phase combination of the same ligand orbital (b_g symmetry) interacts, though more weakly, with the (d_{xy}+) π^* orbital combination (Figure 6). The other most stabilizing interaction involves the highest indene orbital combination of b_u symmetry, III. III finds a metal orbital, the π bonding combination (d_{xz}-) with similar nodal characteristics. As for the above-mentioned interaction, the energy levels of the interacting orbitals are close enough to allow for an important metal contribution to the resulting mo-

(30) Burdett, J. K.; Canadell, E. *Organometallics* **1985**, *4*, 805.

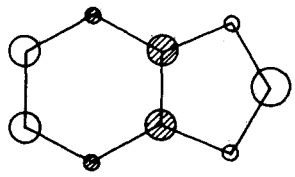

III

lecular orbital. Another stabilizing interaction involves ligand orbital $1b_g$, IV, suited to overlap with the δ metal orbital (d_{yz}+).

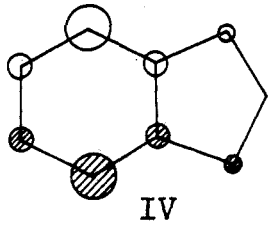

IV

The energy gap between the interacting orbitals is somewhat larger, thus reducing the stabilization energy with respect to the two former strong interactions [0.75 eV, compared to 1.1 eV for the stabilization of both $3b_u$ and $2a_u$ (Figure 6)]. Each of the five underlying ligand π levels is stabilized by less than 0.4 eV. The interactions just discussed are somewhat different from those analyzed by BC for the metal naphthalene dimer, but they compare well with those obtained for M_2 bis(pentalene), in the sense that the three metal levels most destabilized by the strongest metal–ligand interactions are in a similar way π, δ and δ^*.[30]

Let us come now to the results obtained for the present molecule at the ab initio SCF level. As for the other divanadium molecules, the SCF results are somewhat erratic, as can be seen from Table IV. Two closed-shell configurations (^1A_g states) have been characterized. The lowest in energy (−2571.09497 hartrees) corresponds to the $\sigma^2\sigma^{*2}\delta^2\delta^{*2}$ configuration. This configuration has a formal bond order zero between the vanadium atoms. It corresponds to a complete localization of the metal d electrons on their respective metal centers, thus minimizing the correlation effects and accounting for the low SCF energy value. This solution obviously corresponds to an artifact, similar to the nonbonding configuration obtained from RHF calculations on $(Cr_2)^{4+}$ complexes.[31] The second ^1A_g state characterized at the SCF level is 2.25 eV higher in energy. It corresponds to a doubly bonding $\sigma^2\pi^2\delta^2\delta^{*2}$ configuration. This configuration is equivalent to that obtained at the extended Hückel level, in the sense that four δ electrons are localized on the vanadium atoms, whereas two σ and two π electrons are delocalized over both metals. As for the other vanadium complexes, however, the SCF state lower in energy is a quintet state ^5A_g, corresponding to the $\sigma^2\sigma^{*2}\pi^1\pi^{*1}\delta^1\delta^{*1}$ electronic configuration. As for the lowest ^1A_g state, this configuration is nonbonding and minimizes the correlation effects by localizing the electrons. Moreover, the open-shell character of the vanadium atomic configuration partly accounts for Hund's rule prerequisites. This explains the low energy of this configuration (−2.53 eV with respect to the lowest SCF singlet, −4.78 eV with respect to the doubly bonding singlet). However, the nonbonding character of this configuration and its high-spin multiplicity should make it a priori considered as physically unrealistic in spite of the reported paramagnetism of the complex.[19] Intermediate in energy is the lowest triplet state, ^3B_u (−3.04 eV with respect to the doubly bonding ^1A_g state). The electronic configuration is $\sigma^2\sigma^{*2}\pi^2\delta^1\delta^{*1}$, corresponding to a single π bond. As for the quintet state, and at variance from the doubly bonding singlet and from the EH description, the localized electron *pairs* are not accommodated in the δ and δ^* orbitals, *but in the σ and σ^* orbitals*. The contradiction with the EH result can be explained by the fact that

(31) (a) Garner, C. D.; Hillier, I. H.; Guest, M. F.; Green, J. C.; Coleman, A. W. *Chem. Phys. Lett.* **1976**, *41*, 91. (b) Bénard, M.; Veillard, A. *Nouv. J. Chim.* **1977**, *1*, 97. (c) Guest, M. F.; Hillier, I. H.; Garner, C. D. *Chem. Phys. Lett.* **1977**, *48*, 587. (d) Bénard, M. *J. Chem. Phys.* **1979**, *71*, 2546.

Table IV. Energies (Hartrees) Obtained at the ab Initio SCF and CI Levels for Various Configurations of Diindenyldivanadium (3)

state	calc. level	energy[a]	wt %[b]	configuration
^1A_g	SCF	−0.09497	100	$\sigma^2\sigma^{*2}\delta^2\delta^{*2}$
^1A_g	SCF	−0.01210	100	$\sigma^2\pi^2\delta^2\delta^{*2}$
^3B_u	SCF	−0.12390	100	$\sigma^2\sigma^{*2}\pi^2\delta^1\delta^{*1}$
^5A_g	SCF	−0.18803	100	$\sigma^2\sigma^{*2}\pi^1\pi^{*1}\delta^1\delta^{*1}$
^1A_g	CI[e]	−0.38922[c]	51	$\sigma^2\sigma^{*2}\pi^2\delta^2$
^3B_u	CI[e]	−0.37594[d]	70	$\sigma^2\sigma^{*2}\pi^2\delta^1\delta^{*1}$

[a] Shifted by −2571 hartrees. [b] By definition 100% for SCF configurations. [c] −2571.43335 hartrees with Davidson's correction. [d] −2571.41953 hartrees with Davidson's correction. [e] The configuration mentioned in the rightmost column corresponds to the leading term of the expansion.

EH overemphasizes the d–d overlap, as suggested by Woolley,[32] leading to an artificially large σ–σ^* energy gap. This argument does not explain, however, the different localization scheme obtained for SCF closed-shell and open-shell configurations. The sequence of orbital energies obtained for the lowest ^1A_g configuration, in which the σ, δ, δ^*, and σ^* are all doubly occupied, provides an explanation. Orbital energies for the four orbitals are −0.373, −0.305, −0.303, and −0.247 hartree, in that order. Assuming the π orbitals to be doubly occupied in every case, the doubly bonding ^1A_g SCF configuration $\sigma^2\pi^2\delta^2\delta^{*2}$ satisfies the aufbau principle. In the ^3B_u triplet state, the two semioccupied orbitals should develop over the same region of space to take advantage from the localization energy. Two configurations are therefore possible, either $\pi^2\delta^2\delta^{*2}\sigma^1\sigma^{*1}$ or $\pi^2\sigma^2\sigma^{*2}\delta^1\delta^{*1}$. Taking the weighted sum of orbital energies as a stability criterion, the second configuration is more stable by 0.012 hartree, in agreement with the result of the open-shell SCF calculation.

As for the other investigated molecules, the SCF orbitals of the lowest triplet state were taken as a starting orbital set for the iterative CI processing. From the final CI expansions, the covalent singlet appears to be the ground state, lower than the triplet state by 0.0133 hartree (2890 cm^{-1}). Diindenyldivanadium has been reported to be paramagnetic, without additional information concerning the experimental conditions of the magnetic measurement.[19] The calculated S–T separation has the same order of magnitude as the one computed for complex **1** (2820 cm^{-1}), which is reported to exhibit a temperature-dependent singlet–triplet equilibrium.[8] We tentatively assume that the paramagnetism of **3** is due to the similar thermal contamination of a singlet ground state.

The leading configuration of the calculated ^1A_g state in the final CI expansion is $\sigma^2\sigma^{*2}\pi^2\delta^2$ with a weight of 51% (Table I). Note that this leading configuration formally localizes the σ and σ^* electron pairs, as in the triplet SCF configurations and for similar reasons. The second most important configuration (20%) results from a $\delta \rightarrow \delta^*$ two-electron excitation. $\pi \rightarrow \pi^*$ two-electron excitations account for 4% of the CI wave function, and the coefficient of the $\sigma^2\pi^2\delta^2\delta^{*2}$ configuration is less than 0.05. The natural orbital occupations of the singlet and triplet wave functions, along with the metal weight of the singlet NOs, are displayed in Table V.

As a result from an interaction with the LUMO of the indene dimer (**1**), the metal weight in the σ^* NO is no more than 61%, vs 82% for the σ bonding NO (Table V). In spite of the formal localization of the σ and σ^* electrons, the balance for these two electron pairs eventually produces a contribution of ~0.2 to the metal–metal bond order. The delocalization of the σ^* orbital over the indene ligand, as opposed to the high metal character of the σ orbital, appears in Figure 7, displaying the density generated by those orbitals in the xOz plane containing the V–V line and perpendicular to the ligand planes.

A slightly more important contribution to the bond order (~0.3) comes from the δ/δ^* electron pair (respective NO occupations 1.36 and 0.62 e). The most important contribution to the V–V

(32) (a) Woolley, R. G. *Nouv. J. Chim.* **1981**, *5*, 219, 227. (b) Woolley, R. G. *Inorg. Chem.* **1985**, *24*, 3519.

Table V. $(C_9H_7\text{-}V)_2$ (**3**): Population of the Natural Orbitals Obtained for the Lowest Singlet and Triplet States and Metal Character of the NOs for the Singlet Ground State

	orbital popul, e (singlet)	metal, %	orbital popul, e (triplet)
b_g (δ/π^*)	1.98	15	1.98
b_u $(\pi)_{xz}$-	1.98	23	1.98
a_u $(\delta^*)_{yz}$-	1.97	24	1.97
b_u (σ^*)	1.94	61	1.94
a_g (σ)	1.92[a]	82	1.92
a_u $(\pi)_{xy}$-	1.76	74	1.75
a_g $(\delta)_{z^2}$+	1.36	93	1.02
b_u $(\delta^*)_{z^2}$	0.62	97	0.97
b_g $(\pi^*)_{xy}$+	0.21	95	0.22
b_u (σ^*)	0.09	56	0.09
a_g (σ)	0.04	66	0.04
a_u $(\pi)_{xy}$-	0.03	51	0.03

[a] Pairs of bonding/antibonding NOs defined as in Table II.

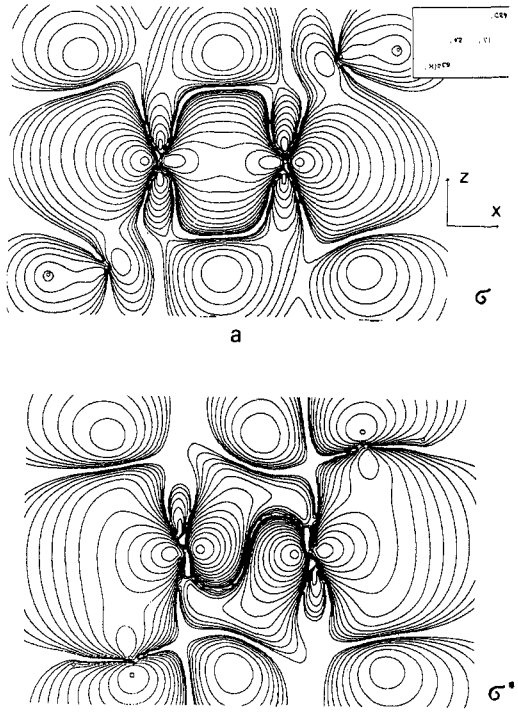

Figure 7. Plot of the electron densities associated with the σ (a) and the σ^* (b) orbitals in $(V\text{-}C_9H_7)_2$ (**3**), in the xOz plane containing the two vanadium atoms and perpendicular to the ligand cycles. The density in two successive contours differs by a factor of 2.

bonding (~0.55), however, comes from the $(\pi_{xy}\text{-})/(\pi^*_{xy}+)$ electron pair, due to the weak population of the antibonding counterpart (0.21 e, Table V). The computed bond order, including the metal contributions from all orbitals, and accounting for the presence of both metal–metal bonding and antibonding contributions in the same representations, is 1.17.

4. $(Cp\text{-}V\text{-}H)_2C_6H_6$ (4). The synthesis and characterization of **4** has been reported by Jonas et al.[20] As for **1**, the centroids of the Cp rings lie away from the V–V axis, opposite to the benzene ring (Figure 1d). The benzene is approximately planar, and each vanadium faces two benzene carbons at 2.15 Å. The V–V distance is 2.425 Å. The hydride atoms could be characterized from X-ray analysis.[20] They are located in the symmetry plane perpendicular to the V–V bond. The V–H and H–H distances are 1.70 and 1.96 Å, respectively, and the H–H axis crosses the symmetry plane containing V–V at 0.66 Å below the metal–metal axis (Figure 1d). This experimental geometry was used for the calculations, slightly modeled to retain the C_{2v} point group.

An orbital interaction diagram between the metal d orbitals of the Cp–V dimer, on the one hand, and the π levels of benzene

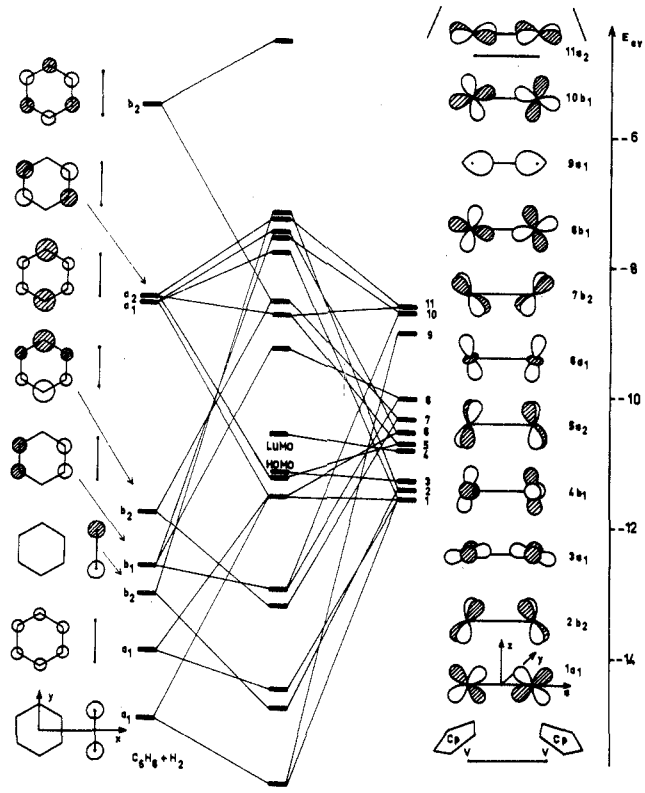

Figure 8. Orbital interaction diagram between the $[V_2(C_5H_5)_2]^{2+}$ fragment and the $[H_2C_6H_6]^{2-}$ moiety leading to molecule **4** (from extended Hückel calculations).

and the σ and σ^* combinations of H_2, on the other hand, is displayed in Figure 8. The diagram is based upon extended Hückel calculations. The Cp rings and the hydride hydrogens, have altogether a formal charge of 4–. The metal is therefore V(II), with three d electrons, and three levels are formally occupied in the representation of the Cp–V dimer given in Figure 8. Both levels of the dihydride, referred to as σ_{H_2} and $\sigma^*_{H_2}$, are also considered as occupied, together with the three lowest π levels of benzene. Sixteen valence electrons should therefore be accommodated into the resulting frontier orbitals.

All five occupied ligand levels display an important stabilization. The metal π bonding orbital of a_1 symmetry (d_{xz}-, level 1 of Figure 8) interacts with both ligand levels of a_1 symmetry, i.e. σ_{H_2} and the totally symmetric π orbital of benzene. The antibonding counterpart of this double interaction should be largely destabilized. This is not the case, however, due to a mixing with the unoccupied benzene orbital of a_1 symmetry. Dimetal level 6, a δ bonding combination of d_{z^2} orbitals, also takes part in this interaction, so that the resulting orbital acquires an important δ character. The other low-lying dimetal orbital with a_1 symmetry is level 3, an orbital with mainly σ bonding character. It remains practically unaffected by the interactions with the ligands and becomes the HOMO of the EH calculation (Figure 8). Similar but still stronger interactions are at work in the b_2 symmetry. The $\sigma^*_{H_2}$ orbital and one benzene level, both formally occupied, belong to this representation. The hydride orbital interacts with dimetal level 2, a combination with mixed π and δ bonding character, spatially well suited to strongly overlap with the out-of-phase combination of hydrogen s lobes. The benzene orbital interacts with level 7 of divanadium, another combination of π and δ bonding orbitals, the lobes of which are now directed toward the bridging carbons of the benzene ring. The destabilization of the antibonding counterpart of this latter interaction is also hindered by an interaction with the highest unoccupied level of benzene, not enough, however, to push the bonding metal orbital down into the occupied set. Finally, the occupied benzene level of b_1 symmetry is somewhat stabilized by two relatively weak interactions with dimetal levels 8 and 10.

Table VI. $(C_5H_5\text{-}V\text{-}H)_2C_6H_6$ (**4**): Population of the Natural Orbitals Obtained for the Lowest Singlet and Triplet States and Distribution of This Population among the Molecular Fragments (from the Mulliken Population Analysis of the Singlet Ground-State NOs)

	orbital popul, e (singlet)	metal, %	H_2, %	C_6H_6, %	Cp, %	orbital popul, e (triplet)
$a_1\ (\pi)_{Bz}$	2.00	8	1	73	17	2.00
$a_1\ (\sigma)_{H_2}$	2.00	17	37	24	12	2.00
$b_2\ (\pi)_{Cp}$	2.00	12	14	21	53	2.00
$a_1\ (\pi)_{Cp}$	1.98	31	9	5	55	1.97
$b_1\ (\pi)_{Bz}$	1.98	20	0	44	36	1.98
$b_2\ (\pi)_{Bz}$	1.98	21	1	54	24	1.98
$b_2\ (\sigma^*)_{H_2}$	1.96	45	33	10	12	1.96
$a_2\ (\delta^*)_{V_2}$	1.85[a]	71	0	26	3	1.84
$a_1\ (\pi)_{V_2}$	1.82	74	2	23	1	1.81
$a_1\ (\sigma/\delta)_{V_2}$	1.41	96	0	2	2	1.01
$b_1\ (\sigma^*/\delta^*)_{V_2}$	0.57	99	0	0	1	0.97
$b_1\ (\pi^*)_{V_2}$	0.15	92	0	7	1	0.17
$b_2\ (\delta)_{V_2}$	0.13	66	24	10	0	0.13
$a_2\ (\pi^*)_{Bz}$	0.04	50	0	48	2	0.06
$a_1\ (\pi^*)_{Bz}$	0.03	45	1	52	2	0.03

[a] Pairs of bonding/antibonding NOs defined as in Table II.

Four frontier levels with predominant metal character either are slightly stabilized or remain energetically unaffected by the metal–ligand interactions. Level 1 is at the center of a complex interaction discussed above, but its energy remains the same as in the Cp–V dimer. Levels 3, of a_1 symmetry, and 4, an antibonding δ^* combination (b_1 symmetry), are unaffected and become the HOMO and the LUMO of the complex, respectively. Level 2 is destabilized. The third occupied metal level arises from the stabilization of level 5, an *antibonding* V–V δ^* combination (d_{yz}-), by the unoccupied benzene orbital of a_2 symmetry (Figure 8). Since one of the three orbitals with major metal weight is antibonding, *the metal–metal bond is formally single.* One should, however, consider that the four most stabilized ligand levels, in representations a_1 and b_2, receive important contributions from metal–metal bonding orbitals leading to a substantial increase of the bond order. The HOMO–LUMO gap is ~0.6 eV only between frontier orbitals lying in similar regions of space. Important correlation effects can therefore be expected once again.

Not all relevant configurations have been investigated at the RHF level. A closed-shell SCF calculation has been carried out on the $(\sigma/\delta)^2\pi^2\delta^{*2}$ configuration, similar to that found at the extended Hückel level. The energy was −2497.55967 hartrees. This energy can be expected to be high relatively to configurations where one or several pairs of d electrons are allowed to relocalize. Indeed, a triplet $^3B_1$ state corresponding to the electronic configuration $(\sigma/\delta)^1(\sigma/\delta)^{*1}\pi^2\delta^{*2}$ was characterized with a SCF energy −2497.72646 hartrees (−4.5 eV with respect to the reference closed-shell configuration). Two quintet configurations, $(\sigma/\delta)^2\pi^1\pi^{*1}\delta^1\delta^{*1}$ and $(\sigma/\delta)^1(\sigma/\delta)^{*1}\pi^2\delta^1\delta^{*1}$, are found to be lower in energy (−2497.75705 and −2497.80062 hartrees, respectively). The gap with the triplet is small, however. The δ orbital (level 2 of Figure 8) is so much destabilized by the metal–ligand interaction that this destabilization energy almost completely offsets the energy recovered from the relocalization of the δ/δ^* electron pair. Other SCF closed-shell and open-shell configurations should yield energies lower than that of the $(\sigma/\delta)^2\pi^2\delta^{*2}$ reference state, but as for the other systems, the orbitals of the triplet $^3B_1$ configuration were taken as a starting point for the CI calculations.

As for the other molecules, the ground state is found to be a singlet, with an energy of −2498.0077 hartrees (−2498.0392 hartrees with Davidson's correction). The leading configuration (55%) is $(\sigma/\delta)^2\pi^2\delta^{*2}$. The second most important configuration (19%) arises from a double excitation from (σ/δ) to $(\sigma/\delta)^*$. Three other configurations, corresponding to crossed excitations from (σ/δ), π, and δ^* to their unoccupied counterparts, globally contribute 7.5%. The individual contributions of all other configurations are less than 1%. A qualitative estimate of the respective contribution of the electron pairs to the correlation effects emerges from the natural orbital populations displayed in Table VI.

Table VII. Comparison of the Characters and Properties of Divanadium Complexes **1–4**

	1	2	3	4
formal bond order	3	2	2	1
computed bond order[a]	1.50	1.15	1.17	1.45
V–V distance, Å	2.439	2.315	2.351	2.425
metal point charge, e	−0.11	−0.28	−0.22	−0.27
S–T energy separation,[b] cm^{-1}	2820	1320	2890	2380
S–T energy separation,[c] cm^{-1}	3580	1380	3000	680
weight of the leading conf, %	43	35	51	55
formal oxidation state of V	II	III	I	II

[a] Defined as $1/2\sum_{MO}[\rho_{V_2}(\text{bonding}) - \rho_{V_2}(\text{antibonding})]$, MO representing all the occupied orbitals including the natural orbitals derived from the CI calculation. [b] From the CI wave function without Davidson's correction. [c] From the CI wave function including Davidson's correction.

Molecules **1–3** could be analyzed in terms of a formal multiple metal–metal bond, but the estimates of the *real* bond orders, as obtained from the metal contributions in each orbital, were less than the formal multiplicity, due to the electron relocalization. The present case is different. The formal bond multiplicity is 1, because of the stabilization of the δ^* orbital (level 5, a_2 symmetry). If the calculation of the real bond order is restricted to the three electron pairs described by the bonding/antibonding orbitals with major metal–metal character, the so-obtained number is 0.35 only, still because of the electron relocalization. But as discussed above, most stabilized ligand orbitals include important contributions from metal–metal *bonding* orbitals. Special emphasis should be given to the case of the formal $\sigma^*_{H_2}$ (b_2 symmetry). The metal contribution to this orbital (45%) appears more important than that of H_2 (33%) (Table VI), in agreement with the well-documented statements that the metal–hydride bond is largely covalent[33] and that the complexed hydrogen atoms do not display a strong hydridic character.[34] Let us note, however, that the Mulliken population of the bridging hydrogens remains significantly higher than 1 electron (1.16 e), at variance from the H populations computed at the ab initio SCF and CASSCF levels for various hydrido carbonyl molecules and ions.[35] The contribution of the σ_{H_2} orbital, and of others, raises the value of the bond order to 1.45, which corresponds to the same order of magnitude as for the divanadium complexes with formally multiple metal–metal bond. As for the other systems, too, the metal contributions to the stabilization of ligand orbitals raise the vanadium point charge to a negative value, −0.27 e in the present case.

The singlet–triplet energy separation computed at the final step of the CI process (not accounting for Davidson's correction) is 2380 cm^{-1}, that is, the same order of magnitude as for **1–3**. At variance from the other systems, however, the accumulated weight of the reference configurations appears noticeably different in the singlet (0.9299) and in the triplet (0.9163) CI wave functions. As a consequence, Davidson's correction drastically reduces the S–T energy gap, from 2380 to 680 cm^{-1}. CI expansions carried out on a given divanadium molecule with different reference spaces have shown that Davidson's estimate of the effect of quadruple excitations could be somewhat erratic, or at least questionable, at this level of approximation. Without questioning the singlet nature of the ground state, it is preferable to warn in the present case that the value of 2380 cm^{-1} probably represents an upper bound to the S–T energy separation.

(33) (a) Low, J. J.; Goddard, W. A., III *J. Am. Chem. Soc.* **1984**, *106*, 6928. (b) Low, J. J.; Goddard, W. A., III *Organometallics* **1986**, *5*, 609. (c) Schilling, J. B.; Goddard, W. A., III; Beauchamp, J. L. *J. Am. Chem. Soc.* **1986**, *108*, 582.

(34) (a) Bursten, B. E.; Gatter, M. G. *J. Am. Chem. Soc.* **1984**, *106*, 2554. (b) Bursten, B. E.; Gatter, M. G. *Organometallics* **1984**, *3*, 896. (c) Berke, H.; Kundel, P. *Z. Naturforsch. B* **1986**, *41*, 527. (d) Berke, H.; Kundel, P. *J. Organomet. Chem.* **1986**, *314*, C31; **1987**, *335*, 353.

(35) Dedieu, A.; Branchadell, V. In *The Challenge of d and f electrons*; Salahub, D. R., Zerner, M. C., Eds., ACS Symposium Series 394; ACS: Washington, 1989; pp 58–76.

Bond Orders and Singlet–Triplet Energy Separations

The four divanadium complexes investigated in the present work could a priori be expected to exhibit extremely different properties. The formal oxidation state of vanadium is respectively II, III, I, and II for **1**, **2**, **3**, and **4**. The formal V–V bond orders deduced from the leading configuration of the ab initio CI expansions are respectively 3, 2, 2, and 1. They correspond to the following electronic configurations: $\sigma^2\pi^2\delta^2$ for **1**, $\sigma^2\delta^2$ for **2**,[36] $\sigma^2\sigma^{*2}\pi^2\delta^2$ for **3**, and $(\sigma/\delta)^2\pi^2\delta^{*2}$ for **4**. In spite of the variety of the formal bonding modes, the observed and computed properties of these complexes, gathered in Table VII, appear strikingly similar.

All metal–metal bond lengths are short, between 2.315 Å for **2** and 2.439 Å for **1**. No correlation can be established between the bond length and the formal bond order. In fact, the longest bond corresponds to the complex with bond order 3. No more correlation appears with the bond orders computed from the CI wave function as

$$\tfrac{1}{2}\sum_{MO}[\rho_{V_2}(\text{bonding}) - \rho_{V_2}(\text{antibonding})]$$

where $\rho_{V_2}(i)$ represents the amount of the population of orbital i that is to be attributed to the dimetal entity according to the Mulliken population analysis. The computed values are surprisingly uniform, between 1.15 and 1.50 (Table VII). The contribution to the bond order of the electron pairs responsible for the through-space V–V bonds is drastically reduced because of the relocalization effects, evidenced by the CI expansion. For **2** and **4**, more than 50% of the computed bond order arises from the stabilizing contribution of V–V bonding combinations to molecular orbitals with formal ligand character. These important metal contributions to several ligand orbitals lead to an increase of the overall metal population. Once again, the metal net charges are strikingly uniform in spite of the different oxidation states of the metal. All types of vanadium atoms have a negative net charge, between −0.1 and −0.3 e (Table VII). The largest point charge (−0.28 e) is obtained for the butanediyl complex **2**. Part of the metal contribution comes, however, from relatively close contacts between the metals and ligand hydrogens. The space partitioning of Mulliken's population analysis may yield in such a case hazardous results. The electron deformation density maps confirm, however, that the metal in all four complexes is in an electron-rich environment compared to the netural, spherical atom.

Coming back to the metal–metal distances, the shortness of the V–V bond lengths does not seem to be a consequence of the direct metal–metal interaction. A feature common to all four complexes is the presence of one metal–metal coupling with δ character. The associated electron pair formally provides one metal–metal bond, but its relocalization on specific metal atoms is so important—almost complete in **2**, slightly smaller in **4**, where the δ coupling is mixed with a significant σ character—that this bond should more adequately be considered as an antiferromagnetic interaction. The presence of a low-lying triplet state, experimentally confirmed for **1**[8] and probably for **3**,[19] is to be related to this weak bond. Except for **4**, a second V–V bond, with σ character, could be characterized from the wave function. The corresponding electron pair also undergoes significant relocalization, more specifically for **3** where an electron pair with σ^* character is also present. The δ and σ bonding orbitals display a high metal weight in all complexes,[37] and the associated bonds can be considered as direct, through-space but weak metal–metal couplings. This is at variance from the π bonds present in **1**, **3**, and **4**, which display ligand contributions of 39%, 26%, and 26%, respectively. The corresponding electron pairs take part in delocalized metal–ligand–metal interactions. The occupation of the associated natural orbitals (1.86, 1.76, and 1.82 e for the bonding NOs, 0.13, 0.21, and 0.15 e for the antibonding ones) indicates that the relocalization on the metal atoms remains moderate, and the contribution to the computed V–V bond order is large. The importance of this delocalized bonding and the metal contribution, already stressed, to the stabilization of a number of ligand orbitals, suggests that the relative position of the metal atoms could be mainly conditioned by their interactions with the bridging ligands. This seems clear for diindenyldivanadium **3** since the metal atoms are facing the ring centroids of the indene ligands without leading to an appreciable deviation from planarity for C_9H_7 (Figure 1c). For $(Cp\text{–}V\text{–}H)_2C_6H_6$ (**4**), the plane defined by a vanadium atom and the two nearest benzene carbons is perpendicular to the V–V axis, a situation quite favorable for the interactions with the π orbitals of benzene (Figure 1d). There is no such geometrical evidence concerning the butanediyl complex (**2**), but ab initio calculations show that the *direct* V–V interactions are especially weak for this molecule and cannot represent the driving force toward a very short metal–metal distance of 2.315 Å. An interpretation of the geometry of **1**, in terms of metal–ligand interactions, appears more difficult since other factors, i.e., repulsive hydrogen contacts between the two Cp rings, seem to be at work.[38] These repulsive interactions can be expected to influence the deviation from planarity of the C_8H_8 ligand, characterized by a dihedral angle of 124°, and to lengthen the metal–metal bond. The V–V distance in **1** is indeed the longest of the four considered molecules at 2.439 Å. The fact that the metal–metal distance could be conditioned by the metal–ligand interactions rather than by the metal–metal ones has been recently advocated in the case of the multiple Cr–Cr bond.[9,39]

A last property that seems to be common to all four complexes is the presence of a low-lying triplet state. The singlet–triplet energy separation represents a very small difference between two large quantities affected by the various approximations of the quantum chemical treatment. This property is therefore difficult to evaluate with quantitative accuracy. A possible approach consists in a perturbative treatment summing out the relatively small number of contributions to the *separation energy* itself, that is, without considering the total energies of the two states. This method has been applied to dinuclear copper complexes.[40] The explicit ab initio/CI calculation of the state energies, at various levels of approximation, has also been applied to transition-metal complexes.[41] The present work is in the line of this latter approach, trying to obtain accurate and consistent values for the energy of both states *at the same high level of approximation.* The consistency between the reference spaces defined for the computation of the singlet and triplet states is therefore essential. This consistency has been defined a priori by the choice of equivalent reference configurations. It can be controlled a posteriori by using as a criterion the accumulated weight of the reference configurations in the CI expansions for the singlet and the triplet states (Table I). These weights should be nearly identical. This criterion is nicely verified for **2** and **3** and with

(36) The frontier orbitals δ and δ^* are quasi degenerate in the extended Hückel treatment (see Figure 4). CI calculations attribute a slightly higher weight to the $\sigma^2\delta^2$ configuration (35.3%, compared to 31.6% for $\sigma^2\delta^{*2}$).

(37) The metal weight is higher than 90% for all σ and δ bonding orbitals, with only one exception (82%).

(38) A deviation of 11.9° from a parallel disposition has been observed between the planes of the Cp rings and the respective fragments of the bridging C_8H_8 ligands and has been attributed to steric interactions between the two C_5H_5 ligands.[7]

(39) (a) Edema, J. J. H.; Gambarotta, S.; van Bolhuis, F.; Spek, A. L. *J. Am. Chem. Soc.* **1989**, *111*, 2142. (b) Edema, J. J. H.; Gambarotta, S.; van Bolhuis, F.; Spek, A. L.; Smeets, W. J. J. *Inorg. Chem.* **1989**, *28*, 1407. (c) Edema, J. J. H.; Gambarotta, S.; Spek, A. L. *Ibid.* **1989**, *28*, 812, and references cited therein. (d) Edema, J. J. H.; Gambarotta, S.; van der Sluis, P.; Smeets, W. J. J.; Spek, A. L. *Ibid.* **1989**, *28*, 3784. (e) Edema, J. J. H.; Gambarotta, S.; Meetsma, A.; van Bolhuis, F.; Spek, A. L.; Smeets, W. J. J. *Inorg. Chem.* **1990**, *29*, 2147.

(40) (a) de Loth, P.; Cassoux, P.; Daudey, J. P.; Malrieu, J. P. *J. Am. Chem. Soc.* **1981**, *103*, 4007. (b) de Loth, P.; Daudey, J. P.; Astheimer, H.; Walz, L.; Haase, W. *J. Chem. Phys.* **1985**, *82*, 5048. (c) Charlot, M. F.; Verdaguer, M.; Journeaux, Y.; de Loth, P.; Daudey, J. P. *Inorg. Chem.* **1984**, *23*, 3802. (d) Daudey, J. P.; de Loth, P.; Malrieu, J. P. In *Magneto-Structural correlations in Exchange Coupled Systems*; Willett, R. D., Gatteschi, D., Kahn, O., Eds.; Reidel: Dordrecht, 1984. (e) Astheimer, H.; Haase, W. *J. Chem. Phys.* **1986**, *85*, 1427. (f) Nepveu, F.; Haase, W.; Astheimer, H. *J. Chem. Soc., Faraday Trans. 2* **1986**, *82*, 551.

(41) (a) Broer, R.; Maaskant, W. J. A. *Chem. Phys.* **1986**, *102*, 103. (b) Demuynck, J.; Mougenot, P.; Bénard, M. *J. Am. Chem. Soc.* **1987**, *109*, 2265. (c) Rohmer, M.-M.; Grand, A.; Bénard, M. *J. Am. Chem. Soc.* **1990**, *112*, 2876. (d) Rohmer, M.-M.; Bénard, M. *Organometallics* **1990**, in press.

good approximation for **1** (Table I). As a consequence, the estimate of the effect of quadruple excitations (Davidson's correction) does not heavily modify the energy difference (Table VII). For system **4**, the weight of the reference configurations is significantly higher for the singlet than for the triplet state (Table I) and Davidson's correction strongly reduces the S-T difference from 2380 to 680 cm^{-1}. A more extended CI calculation or a perturbative estimate should be necessary to refine this latter value.

The S-T separation for **1** has been estimated from NMR spectroscopy as 22-24 kJ mol^{-1},[8] that is, 1840-2000 cm^{-1}, in reasonably good agreement with the value computed in the present work (2820 cm^{-1}).

Conclusion

Four binuclear complexes of vanadium assumed from electron counting considerations to exhibit strikingly different electronic structures affecting the dimetal unit have been investigated by means of a multistep ab initio CI treatment. It appears from the calculations that in spite of different V-V bond orders, varying from 1 to 3, the four complexes share several characters and properties, such as a slightly negative net charge for the metal atoms, a computed bond order between 1.15 and 1.50, and the presence of a low-lying triplet state at less than 3000 cm^{-1} above the singlet ground state. These computed similarities should be compared to the relatively short range of the V-V distanced between 2.315 and 2.439 Å. The calculations show that two types of contributions to the metal-metal interaction should be considered. On the one hand, weak, direct interactions of the δ and σ types are responsible for the small singlet-triplet energy gap. Due to an important relocalization effect evidenced from the natural orbital occupation numbers, those interactions give little contribution to the computed bond order. On the other hand, delocalized metal-ligand-metal interactions with V-V bonding character are present in all four complexes. These interactions may either correspond to formal metal-metal bonds as in **1** and **3** or result from the stabilization of ligand orbitals by V-V bonding orbital combinations as in **2** and **4**. The resulting orbitals are little affected by correlation effects, and the metal contribution therefore remains bonding and delocalized. These MOs provide an important contribution to the computed V-V bond order. The electronic structure of the dimetal subunit that can be formally deduced from electron counting considerations is therefore subject to important corrections in opposite directions. On the one hand, relocalization of through-space metal-metal bonding electrons considerably reduces their contribution to the bond order. On the other hand, delocalized electrons that should be in most cases formally attributed to the ligands do provide the largest share of the metal-metal bonding. Relocalization prevails for complexes with formal multiple V-V bonds (**1**, **2**, and **3**), and the formal bond order is reduced by a factor close to 2. In contrast, delocalized bonding raises the bond order of **4** from 1, the formal value in the leading configuration, to 1.45. The result is an equalization of the electronic properties of the four complexes and a greater sensitivity of the structural parameters to the metal-ligand rather than to the metal-metal interaction.

Acknowledgment. We are pleased to thank Pr. C. Krüger and Dr. R. Goddard for a stimulating discussion. All calculations have been carried out on the CRAY-2 computer at the CCVR (Palaiseau, France) through a grant of computer time from the Conseil Scientifique du Centre de Calcul Vectoriel de la Recherche.

Registry No. **1**, 107201-40-1; **2**, 104462-69-3; **3**, 104598-74-5; **4**, 86421-59-2.

Electron Propagator Theory of the Ground and Excited States of $CaBH_4$

J. V. Ortiz

Contribution from the Department of Chemistry, University of New Mexico, Albuquerque, New Mexico 87131. *Received August 13, 1990*

Abstract: Electron propagator theory provides a correlated one-electron picture of bonding in various states of $CaBH_4$. Calculations of $CaBH_4^+$ electron affinities produce ground- and excited-state energies at the optimized, C_{3v} minimum of the neutral ground state and at a C_{2v} geometry. Contour plots and expectation values of Feynman-Dyson amplitudes (FDA's) describe the distribution of the least bound electron in various states. $\tilde{X}^2A_1$ has an unpaired electron in a Ca sp hybrid polarized away from BH_4. Splittings of Ca d orbitals, variable hybridization with Ca p orbitals, and contrasting Ca-ligand bonding properties characterize the next few states, which display π, σ, and δ pseudosymmetry in their FDA's. The splitting of the first two excited states is not as large as it is in calculations where BH_4 is replaced by a ligand which confronts Ca with a lone pair of electrons with σ pseudosymmetry. Higher excited states have electrons in diffuse orbitals that have been orthogonalized to the bonding regions.

I. Introduction

Many radicals composed of Ca and a ligand with a positive electron affinity have a single electron localized about Ca. Several spectroscopic investigations of $C_{\infty v}$ examples have confirmed this simple picture, where several orbitals with σ, π, or δ symmetry, often exhibiting considerable mixing among metal s, p, and d orbitals, can accept the least bound electron.[1-3] When the ligand is not linear, for example, NH_2 or CH_3, cylindrical pseudosymmetry, defined by an axis connecting Ca to the other non-hydrogen nucleus, remains useful as an organizing principle.[4] Even for a linear ligand entering into a nonlinear arrangement with Ca, as in CaSH, this scheme retains its qualitative validity.[5] $CaBH_4$ is unlike previously studied molecules in that the ligand does not present the metal with a single lone pair of electrons with σ pseudosymmetry. Borohydride anion generally binds to metal

(1) Nakagawa, J.; Domaille, P. J.; Steimle, T. C.; Harris, D. O. *J. Mol. Spectrosc.* **1978**, *70*, 374. Dulick, M.; Bernath, P. F.; Field, R. W. *Can J. Phys.* **1980**, *58*, 703. Bernath, P. F.; Field, R. W. *J. Mol. Spectrosc.* **1980**, *82*, 339.

(2) Wormsbecher, R. F.; Trkula, M.; Martner, C.; Penn, R. E.; Harris, D. O. *J. Mol. Spectrosc.* **1983**, *97*, 29. Hilborn, R. C.; Qingshi, Z.; Harris, D. O. *J. Mol. Spectrosc.* **1983**, *97*, 73. Bernath, P.; Kinsey-Nielsen, S. *Chem. Phys. Lett.* **1984**, *105*, 663. Bernath, P. F.; Brazier, C. R. *Astrophys. J.* **1985**, *288*, 373.

(3) Ellingboe, L. C.; Bopegedera, A. M. R. P.; Brazier, C. R.; Bernath, P. F. *Chem. Phys. Lett.* **1986**, *126*, 285. Bopegedera, A. M. R. P.; Brazier, C. R.; Bernath, P. F. *Chem. Phys. Lett.* **1987**, *136*, 97. Bopegedera, A. M. R. P.; Brazier, C. R.; Bernath, P. F. *J. Mol. Spectrosc.* **1988**, *129*, 268. Brazier, C. R.; Bernath, P. F. *J. Chem. Phys.* **1988**, *88*, 2112.

(4) Ortiz, J. V. *J. Chem. Phys.* **1990**, *92*, 6728.

(5) Ortiz, J. V. *Chem. Phys. Lett.* **1990**, *169*, 116.

0002-7863/91/1513-1102$02.50/0